Fuel 183 (2016) 177–184

Contents lists available at ScienceDirect

Fuel

journal homepage: www.elsevier.com/locate/fuel

Full Length Article

An advanced biomass gasification technology with integrated catalytic hot gas cleaning. Part III: Effects of inorganic species in char on the reforming of tars from wood and agricultural wastes

Shu Zhang [a], Yao Song [a], Yun Cai Song [a,b], Qun Yi [a,b], Li Dong [a], Ting Ting Li [a], Lei Zhang [a], Jie Feng [b], Wen Ying Li [b,*], Chun-Zhu Li [a,*]

[a] Fuels and Energy Technology Institute, Curtin University of Technology, GPO Box U1987, Perth, WA 6845, Australia
[b] Key Lab of Coal Science and Technology, Taiyuan University of Technology, Taiyuan 030024, PR China

HIGHLIGHTS

- The raw and H-form char were used to reform tar in a pilot scale gasifier.
- The effects of inorganics in the char catalyst on tar reforming were obvious.
- The catalyst also captured volatilised inorganics from raw gasification gas.

ARTICLE INFO

Article history:
Received 5 March 2016
Received in revised form 10 May 2016
Accepted 16 June 2016

Keywords:
Biomass
Gasification
Tar reforming
Char
Catalysts
AAEM species

ABSTRACT

Char is used directly as a catalyst for the catalytic reforming of tar during gasification. Experiments have been carried out to examine the effects of inorganics in char as a catalyst for the catalytic reforming of tar during the gasification of mallee wood, corn stalk and wheat straw in a pilot plant. The char catalyst was prepared from the pyrolysis of mallee wood at a fast heating rate. The catalytic activities of char and acid-washed char for tar reforming were compared under otherwise identical gasification conditions. For all biomass feedstocks tested for gasification, the tar contents in product gas could be drastically reduced by the catalyst, reaching a tar concentration level well below 100 mg/N m^3. The acid-washed char also showed profound activity for tar reforming although its catalytic activity was definitely lower than the raw char. Both catalysts could effectively reform the aromatic ring systems (especially large aromatic ring systems with three or more fused benzene rings) in tars as is revealed using UV-fluorescence spectroscopy. The char itself was also partially gasified. After being used as a catalyst, the condensation of the aromatic rings and the accumulation of inorganic species led to drastic changes in char reactivity with O_2 at 400 °C. The inorganic species in char tended to enhance the formation of H_2 and CO during the reforming reactions in the catalytic reactor.

1. Introduction

Biomass, as one of the main renewable energy resources, is abundantly available worldwide, especially in remote areas where electricity grid network may not necessarily cover. The gasification of local biomass feedstock combined with a gas engine could be an economically viable and environmentally friendly option for distributed electricity generation. Due to its high reactivity, biomass will immediately decompose into volatiles and char once it is fed into a hot reactor. The contact between the highly reactive volatiles and char could considerably inhibit the reaction rate of char and gasifying agents inside a gasifier [1–6]. Furthermore, the volatiles would consume the gasifying agents (e.g. oxygen and steam) at a much higher rate than char, which again is undesirable in terms of char conversion and gasification efficiency. It is therefore highly desirable to minimise the volatile-char interactions and to optimise the volatile-oxygen reactions inside the gasifier, which could be potentially realised by our recently proposed gasification technology [3,4,7].

Tar reduction is a well-recognised roadblock in the commercialisation of advanced biomass gasification technologies. A variety of catalysts such as dolomite, olivine and Ni—Al_2O_3 catalysts have

* Corresponding authors.
E-mail addresses: ying@tyut.edu.cn (W.Y. Li), chun-zhu.li@curtin.edu.au (C.-Z. Li).

http://dx.doi.org/10.1016/j.fuel.2016.06.078
0016-2361/

been tried for tar removal [8–11]. These catalysts have high activities to reform tar, but they are expensive and easily lose their activities due to the coke deposition. Our studies [12–18] have shown that char and char-supported catalysts could be an ideal candidate to substantially reform the tarry material. Based on these studies, our technology will use char or char-supported catalysts to reform tar [3,7]. The feasibility of tar removal using char or char-supported catalysts has been demonstrated in our pilot plant [3,4].

The active sites in the char catalysts for tar reforming were mainly attributed to the carbon structure as well as the inorganic species in char. Alkali and alkaline earth metallic (AAEM) species can be abundant in biomass and become important catalysts in char for tar reforming. Unfortunately, AAEM species [19–24] undergo drastic transformations during pyrolysis and gasification. Their concentrations and chemical forms would vary significantly with the pyrolysis and gasification conditions under which the char catalyst is prepared. The studies using small amounts (<a few grams) of char [5,12–18] would provide fundamental understanding on the reactions taking place during the catalytic reforming of tar using char catalysts. The inherently-existing and externally-loaded AAEM in char may not only play key roles in tar reduction but also affect compositions of light gases (H_2, CO, CO_2 and CH_4). Therefore, trials in a pilot plant are essential to answer these fundamentally important questions.

This study aims to investigate the effects of inorganic species on the catalytic reforming of tar in a pilot plant. The char (catalyst) was prepared from the pyrolysis of mallee wood at fast heating rates. The char was also washed with acid to remove inorganic species. Our results indicate that the AAEM-laden char can have higher catalytic reactivities than the corresponding AAEM-lean char. AAEM species also affect the product gas compositions.

2. Experimental

2.1. Biomass samples

Three different biomass samples (mallee wood, wheat straw and corn stalk) were chosen as feedstock for the gasification experiments. Mallee wood and wheat straw were grown in Western Australia. Corn stalk was obtained from Shanxi Province in China. All the biomasses were sized to the range of 0–6 mm and further dried at 105 °C for 10 h in an oven. The dried biomass samples containing 3–5 wt% moisture due to the transfer from oven to biomass hopper were then ready for use. The proximate and ultimate analyses of biomass are listed in Table 1 and the AAEM contents (Na was negligible) in the biomass are shown in Table 2.

2.2. Gasification experiments

A lab-scale gasification pilot plant that has been described in detail in previous publications [3,4] was used for conducting the gasification experiments. All experiments were operated at slightly above the atmospheric pressure to maintain the required gas flows. Briefly, 3 pairs of cones as internal structure were purposely built inside the reactor (H1.50 m × Φ0.44 m) to increase the residence time of biomass particles in the reaction zone as well as to improve the heat transfer to the biomass particles. A catalytic reactor (H0.5 m × Φ0.16 m) was integrated with the top of the gasifier. The gaseous products including tarry compounds from gasification had to travel through the catalytic reactor where the condensable hydrocarbons would be considerably reformed into light and clean product gases. To ensure identical GHSV when the gas products went through the char catalysts bed, the char catalysts were always over loaded (~1.5 kg) to ensure that the outlet of catalytic reactor was fully covered during the experiments. The outlet of catalytic reactor was located at the side of cylindrical catalyst reactor while the catalysts could be loaded into the reactor from its top. The configuration of the catalytic reactor could be easily found in Part I of this series of study. The temperature distribution inside the gasifier from the top to the bottom has been plotted and shown in Part I of this series of study. The average temperatures in the main gasifier reactor and catalyst chamber are ~880 °C and 800 °C respectively. The ratios of steam to biomass and oxygen to biomass were kept the same as previous studies, namely 0.59 kg/kg and 45 L/kg respectively. The flow rates of O_2 and N_2 were accurately controlled by a mass flow controller and a rotary flow meter respectively. The mixture of O_2 and N_2 entered into the reaction zone from the bottom of gasifier while the steam was supplied from the side bottom of gasifier by injecting a prescribed flow of water through a high precision peristaltic pump.

To determine the tarry materials in gas products, two sampling tubers were installed just before and after the catalysts bed, enabling that a stream of gas could be collected from the hot region (>330 °C) before and after the catalysts bed respectively at 2 L/min for 10 min for each sample. The hot gas would pass through a series of bubblers (impingers) filled with a mixture of chloroform and methanol (4:1 by vol.) which were placed in a dry ice bath (−78 °C) for condensing the tar out of the product gas. After the condensing unit, the permanent gases flew into a rotary flow meter and then went into an on-line gas analyser (ABB). There was a pump integrated inside the gas analyser, which facilitated the control of gas flow rate.

After experiments, the spent catalysts from the reaction zone rather than those above the reactor outlet were collected for further analysis.

2.3. Catalyst preparation

The bio-char catalysts used in this study were prepared from the pyrolysis of mallee wood at fast heating rates in the gasification plant itself. 30 kg of mallee chips (6–10 mm) were fed into the hot reactor at a feeding rate of 20 kg/h at a temperature of 600–950 °C. Due to the specially-designed internal structure, the biomass particles would immediately drop on the hot surface of the first cone and move down in an "S" shape. The contact with the hot stainless steel greatly enhanced the fast heating rate experienced by the biomass particles. 3 L/min nitrogen was continuously supplied from the bottom of the reactor to ensure an inert atmosphere for the biomass decomposition and the growing char (catalysts) bed. At

Table 1
Property of biomass feedstock.

Biomass	Ash	Volatile	C[b], %	H[b], %	O[c], %	N[b], %	S[b], %
	Yield[a], %	Matter[b], %					
Corn stalk	14.2	82.5	49.3	6.0	43.3	1.0	0.4
Wheat straw	6.5	79.8	48.6	6.5	*43.2*	1.5	0.2
Mallee wood	0.9	81.6	48.2	6.1	45.5	0.2	0.0

[a] Dry-basis.
[b] Dry-ash-free basis.
[c] By difference.

Table 2
AAEM contents (dry basis) of biomass feedstock.

Biomass	K, %	Mg, %	Ca, %
Corn stalk	1.51	0.24	0.33
Wheat straw	1.16	0.06	0.13
Mallee wood	0.06	0.03	0.15

the end of the experiment, the reactor was naturally cooled down under the protection of nitrogen. The catalyst (~4.0 kg) was successfully collected by opening the bottom flange of the reactor. It was then sieved to obtain the 4–6 mm size range used in this study. The prepared catalyst (4–6 mm) was hereafter named as raw catalyst (named as R-catalyst hereafter).

Another type of catalyst used in this study was prepared by acid-washing the raw catalyst. Highly concentrated sulphuric acid was first diluted to 0.2 M in double distilled water. The R-catalyst was then soaked into the acid solution in the mass ratio of 1:30 for 72 h. The acid-washed catalyst (referred to as the H-catalyst indicating that the majority of AAEM species were replaced by H in the acid) was then obtained by filtration, water washing and drying (60 °C). The K, Mg and Ca contents in the H-catalyst were 0.04, 0.15 and 0.50 (wt%, db), compared to 0.42, 0.19 and 1.16 (wt%, db) in the R-catalyst. More than 90% of K as the key catalytic species in biochar has been successfully removed.

Following our previous experiments [3,4], the catalyst was always activated in situ at 800 °C in the catalyst bed by steam prior to the feeding of biomass to commence the gasification experiments. The activating time was 10 min.

2.4. Tar content determination using combustion method

As detailed in Part I [3] of this series of work, the quantity of tar collected in the mixed solvent was determined by the combustion method due to the fact that the tar mass was too small to be weighed accurately. Briefly, a portion of tar solution in an aluminium tray was firstly dried at 35 °C in an oven for 12 h to evaporate all solvents. The organic residue sticking to the aluminium tray was then completely combusted in a two-stage quartz reactor where the tar evaporated in an inert atmosphere at 600 °C on the top stage and the evaporated tar flew down to the bottom stage and was burned in oxygen at 900 °C. The produced CO_2 with excessive O_2 was all collected in a 20 L gas bag. Its CO_2 concentration was determined by a GC. Therefore, the amount of tar actually refers to the mass of carbon in the tar.

2.5. Tar analysis using UV-fluorescence spectroscopy

UV-fluorescence spectra of the diluted tar samples (4 ppm) in methanol were recorded in a Perkin–Elmer LS50B luminescence spectrometer with 1 cm light path length [3,4]. The methanol was spectroscopy grade with purity (GC) of ⩾99.9%. The synchronous spectra were recorded with a constant energy difference of −2800 cm^{-1}. The slit widths were 2.5 nm while the scan speed was 200 nm/min. Each sample was scanned four times to obtain a sound quality spectrum. For the purpose of comparison based on the biomass mass, the fluorescence intensity was expressed on the basis of "per kg of biomass" [3].

2.6. Catalyst characterization

2.6.1. AAEM species

AAEM concentrations in catalysts were quantified based on a previously established procedure [4,19]. Briefly, the catalyst samples in platinum crucibles were first ashed in a muffle furnace. The ash together with the crucible was then digested in HF and HNO_3 acids (1:1 ratio) in Teflon vials for 16 h. The acid mixture was then evaporated and 2% nitric acid (Suprapur, 65%) was added to the sample vials to dissolve the residue. The AAEM species in the acid solution were quantified using a Perkin-Elmer Optima 7300DV ICP-OES spectrometer.

2.6.2. Carbon structure

A Perkin-Elmer Spectrum GX FT-IR/Raman spectrometer was used to record the Raman spectra of the catalysts before and after being used. The methods have been detailed previously [4,5]. Basically, the catalyst (char) sample was firstly diluted to 0.25 wt% with IR grade KBr and then ground for 10 min. The mixed fine particles (100 mg) were then packed into a cylindrical shape in a sample holder. The excitation laser wavelength was 1064 nm with a nominal laser power of 150 mW. The spectral resolution was 4 cm^{-1}. 10 Gaussian bands were used to deconvolute the original Raman spectra. Among them, D (1300 cm^{-1}) band reflects the highly aromatised structure (no less than 6 fused aromatic rings) while G_R (1540 cm^{-1}), V_L (1465 cm^{-1}) and V_R (1380 cm^{-1}) bands together denote small aromatic ring systems in amorphous carbon structure.

2.6.3. Combustion reactivity

The reactivity of catalysts with O_2 was measured using a Perkin-Elmer Pyris1 thermogravimetric analyser (TGA) following the previously-established method [6,25]. About 5 mg of a catalyst was loaded into a sample pan and heated from ambient to 110 °C in nitrogen (Ultra High Purity) and held for 30 min in order to fully remove moisture. The sample was further heated to 400 °C at the rate of 50 °C/min in nitrogen. After keeping at 400 °C for 2 min, the atmosphere was switched to air and the reactivity measurement started. The reactivity, R, was calculated by:

$$R = -\frac{1}{W}\frac{dW}{dt}$$

where W is the catalyst weight (dry-ash-free basis) at any given time t.

At the last step of the temperature programme, the temperature was increased to 600 °C and held for 30 min in order to burn off any remaining carbonaceous material. The resultant mass was considered as the weight of ash.

3. Results and discussion

3.1. Effects of catalysts on tar reforming

3.1.1. Tar contents in product gas

Fig. 1 shows the tar contents in product gases from the gasification of three types of biomasses; the gas sampling points were located before and after the catalyst bed. By comparing the datum points on the top and bottom parts in Fig. 1, it is clearly seen that the tar contents in the product gas have been remarkably reduced

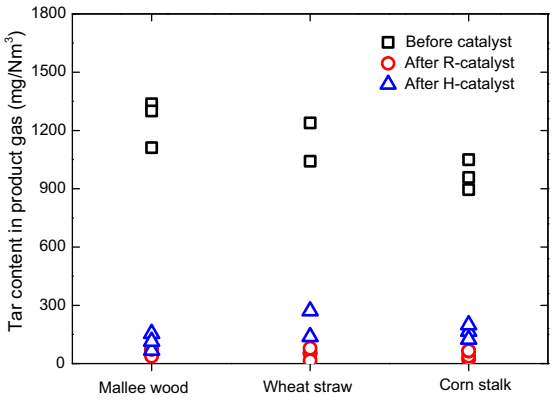

Fig. 1. Tar contents in the product gases collected before and after the R- and H-catalyst beds during the gasification of different biomasses.

by the use of R- or H-catalyst. Specifically, all the product gases after passing through R-catalyst contained the tar well below 100 mg/N m^3, which is the upper limit for the product gas to be burned in a gas turbine or engine without causing severe problems [26,27]. The difference in tar contents before catalyst beds among various feedstock could be observed. However, the variation in tar contents after the catalytic reforming tended to diminish, demonstrating the high suitability of the catalysts for a wide range of biomass feedstock.

The char or char-supported metal species as catalysts for reforming organic compounds in product gas from pyrolysis and gasification has been reported previously [3,4,12–18], though mostly from bench scale studies. As was expected, the presence of inorganic species (particularly K) in the char has enhanced the tar reduction during the reforming reactions. The tar content in the gas reformed by the R-catalyst was around 50 mg/N m^3 while the product gas still contained about 150 mg/N m^3 tar after being reformed by the H-catalyst. The potassium well-dispersed in the char matrix could considerably catalyse the decomposition and gasification of hydrocarbons, facilitating the tar reforming.

The activity of H-catalyst shown in Fig. 1 appears to differ from the results obtained by Min [15] who concluded that the char from H-form coal showed very poor reactivity for tar reforming. However, the char used in this study was derived from the pyrolysis of biomass instead of coal, and the bio-char matrix featured a totally different carbon structure from that of the coal char. The importance of carbon structure for char as a reforming catalyst has been addressed in our Part II and in another study [17] that compared catalytic performances of different chars, among which bio-char-based catalysts did produce much lower tar contents than the coal char. Biomass char structure is highly amorphous with numerous defects and unstable chemical bonds. The defects in the carbon structure of H-catalyst could thus act as reactive sites for tarry compounds to anchor and reform. In addition, the role of steam that was always present in the volatiles during the tar reforming should not be forgotten as it could directly reform the tar compounds and/or indirectly play roles by varying volatile-char interactions [18]. The good activity of H-catalysts is also technically important in practical applications. Our data in Fig. 1 generally indicate that biochars even containing very limited AAEM can still act as a potential catalyst for tar reforming.

3.1.2. Aromatic ring systems in tar revealed by UV-fluorescence spectroscopy

The tar in the product gas from gasification reactions consists mainly of aromatics with various fused sizes. The aromatic ring systems could condense and/or possibly polymerise into solid at elevated temperatures, which is a key issue in the utilisation of the product gas containing tarry materials, e.g. in a gas turbine or engine. UV fluorescence spectroscopy has been employed as a useful and delicate tool to provide information on the aromatic ring systems in tars from the pyrolysis and gasification of coal and biomass [3,4,14,15]. To minimise the possible self-absorption and inter-molecular energy transfer, tar samples were further diluted to 4 ppm in UV grade methanol for collecting the constant energy synchronous spectra.

Fig. 2 exhibits changes in aromatic ring systems in the tars from the gasification of three biomasses in the presence and absence of catalysts. The most striking feature shown in Fig. 2 is the reduction in the fluorescence intensity of tars before and after being reformed using the char as a catalyst for any given biomass feedstock. This observation is consistent with that on the tar contents measured using the combustion method as shown in Fig. 1. The large aromatic ring systems (e.g. corresponding to the wavelengths >360 nm) were reformed much more significantly than the small aromatic ring systems. The large size of aromatic rings likely contained reactive branches/links, such as oxygenated/aliphatic groups, while the isolated small aromatics such as naphthalene were relatively stable [18]. Additionally, the large aromatic rings might be advantageous to the adsorbing process on the catalysts surface, thus enhancing its reforming reactions.

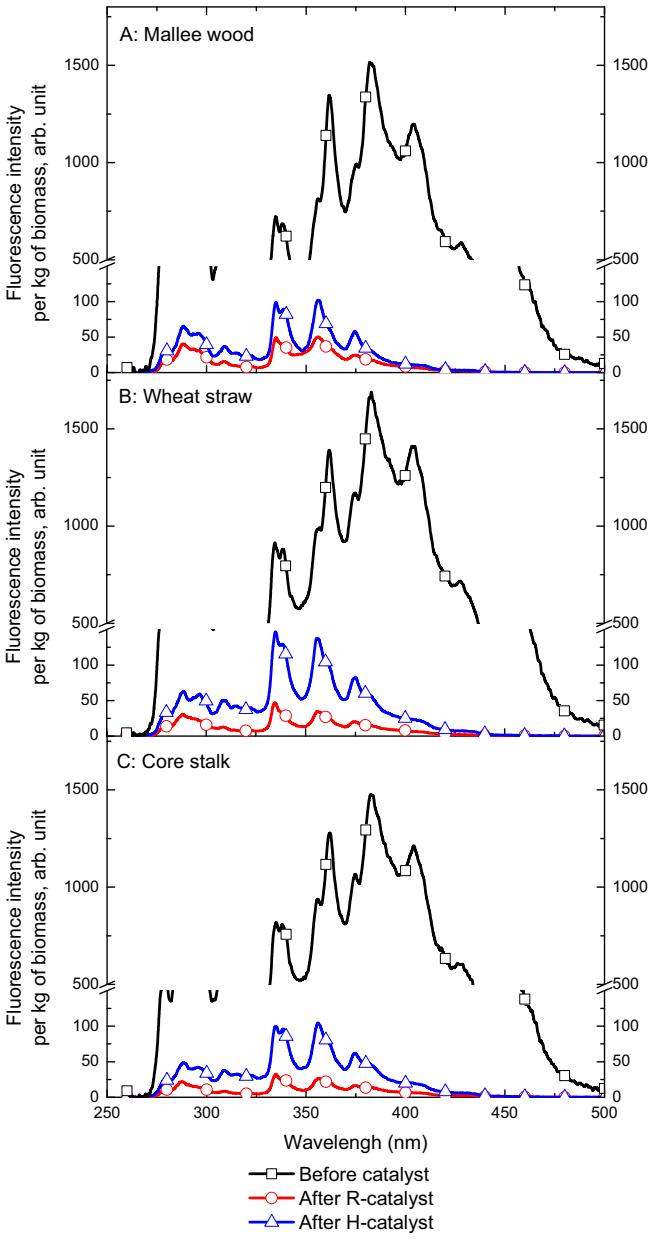

Fig. 2. Constant energy synchronous spectra of tar solution (−2800 cm^{-1}). (A) The tar was produced from mallee wood gasification; (B) the tar was produced from wheat straw gasification; (C) the tar was produced from corn stalk gasification.

Although the relative percentage of small aromatic ring systems in the reformed tar was much higher than that in the tar before passing through the catalysts bed, the small aromatic compounds were indeed considerably eliminated because the fluorescence intensity of tars before and after reforming differed by approximately a factor of 10 times. The reforming reaction for the small aromatic ring systems may be much more severe than observed, considering that the reforming of those large aromatics might form some small aromatics. Clearly, Fig. 2 also indicates that AAEM species in the catalysts (R-catalyst versus H-catalyst) were shown to enhance the reforming of tar in each case.

3.2. Effects of catalysts on product gas compositions

Gas composition is another paramount factor for evaluating gasification technologies as it determines the quality (such as ratio of H_2:CO and heating value) and the potential applications of the gas products. Fig. 3 shows the changes in gas composition (A: H_2, B: CO, C: CO_2, D: CH_4) before and after R-catalyst during the gasification using different biomasses, whereas the gas compositions after R- and H-catalysts are compared in Fig. 4.

From Fig. 3, the reforming reactions in R-catalyst bed have enhanced the formation of H_2 and CO while CO_2 and CH_4 have dropped correspondingly. Overall, the partial gasification of tarry materials and char (catalysts), WGS (water-gas-shift) reactions, methane reforming reactions as well as the condensation reactions of large aromatics were together responsible for the eventual variations in the gas compositions. The fluctuation of data points in Fig. 3 does not allow us to conclude the exact trends for the effects of feedstock on the gas compositions although the CO and H_2 contents from mallee wood gasification may be somewhat higher than those from wheat straw and corn stalk gasification. The insignificant differences in gas compositions due to the use of different feedstocks further suggested the low dependency of gas quality on feedstock selections for the gasifier. In other words, Figs. 1 and 3 indicate that the gas quality from mallee wood, wheat straw and corn stalk were broadly similar.

From Fig. 4, the product gas collected after H-catalyst contained higher percentages of CO_2/CH_4 and lower percentages of H_2/CO than that after R-catalyst, further supporting that the catalyst-gas reactions in the H-catalyst bed were less significant than those in the R-catalyst bed. The lack of AAEM in the H-catalyst has obviously reduced its catalytic activity for tar reforming reactions, thus affecting the tar contents, tar composition and gas composition as shown in Figs. 1–4.

3.3. Changes in catalyst before and after use

3.3.1. Carbon structure

Fig. 5 shows the changes in the carbon skeletal structure of the catalysts before and after being used, which is revealed by FT-Raman spectroscopy. As introduced in Section 2, the value of $I_{(GR+VL+VR)}/I_D$ could actually reflect the ratio of small to large aromatic ring systems in the amorphous carbon structure of catalysts (chars), whereas the total Raman area is mainly determined by the extent of aromatic ring condensation and the abundance of O-containing functional groups [4,5].

Compared to the fresh catalysts, the ratio of small to large aromatic ring systems in the spent catalysts clearly reduced as shown in Fig. 5(a), which well agreed with our previous report [4] although the catalysts (chars) used in the two studies were prepared from different heating rates. The increase of aromatisation in catalysts was well expected as volatile-char interactions and steam gasification took place simultaneously with the reforming reactions. The volatile-char interactions have been intensively demonstrated to generate radicals (especially H radicals) and enhance the size of fused aromatic rings [1,2,5]. Char-steam reactions in the catalyst bed also intended to preferentially remove the small and reactive aromatic ring systems [4,6,28].

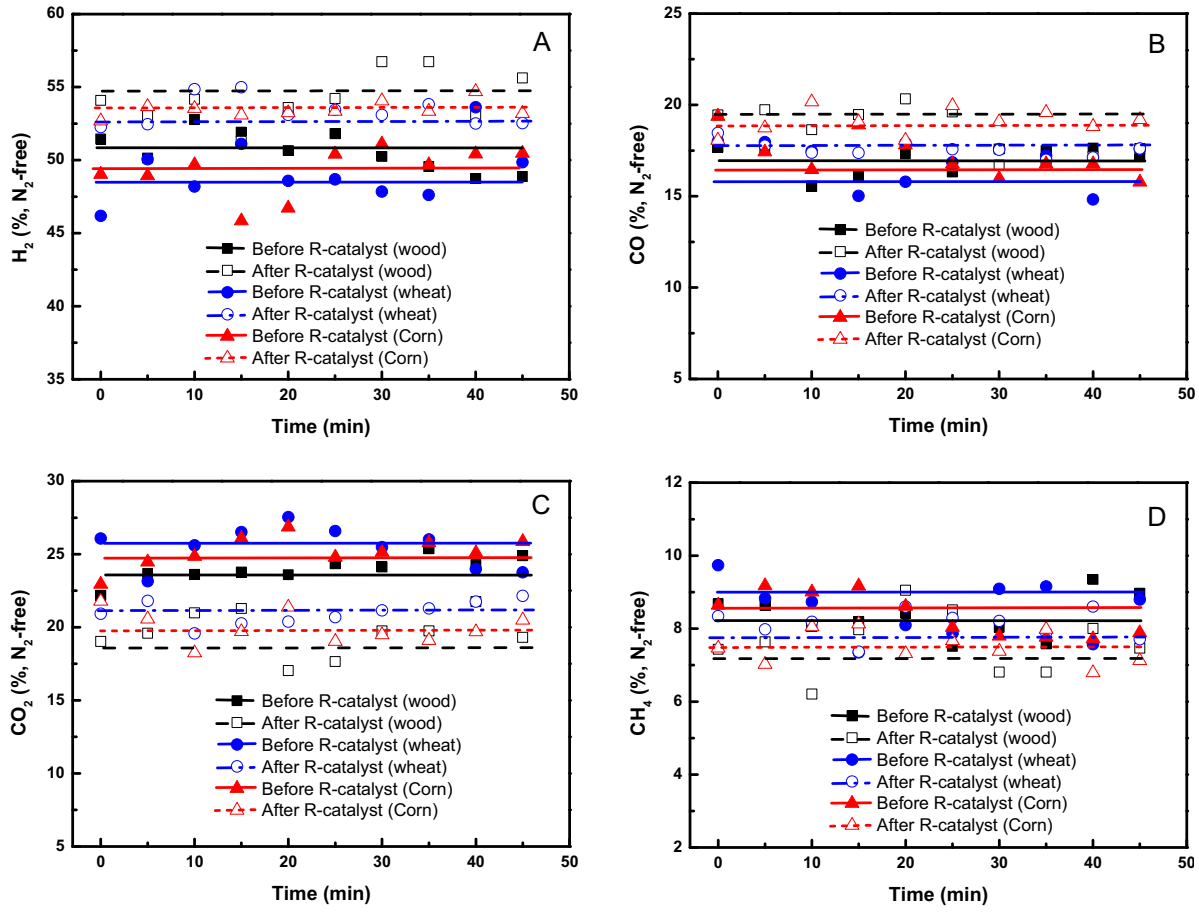

Fig. 3. Gas compositions on the dry and N_2-free basis in the absence and presence of R-catalyst using different gasification feedstock.

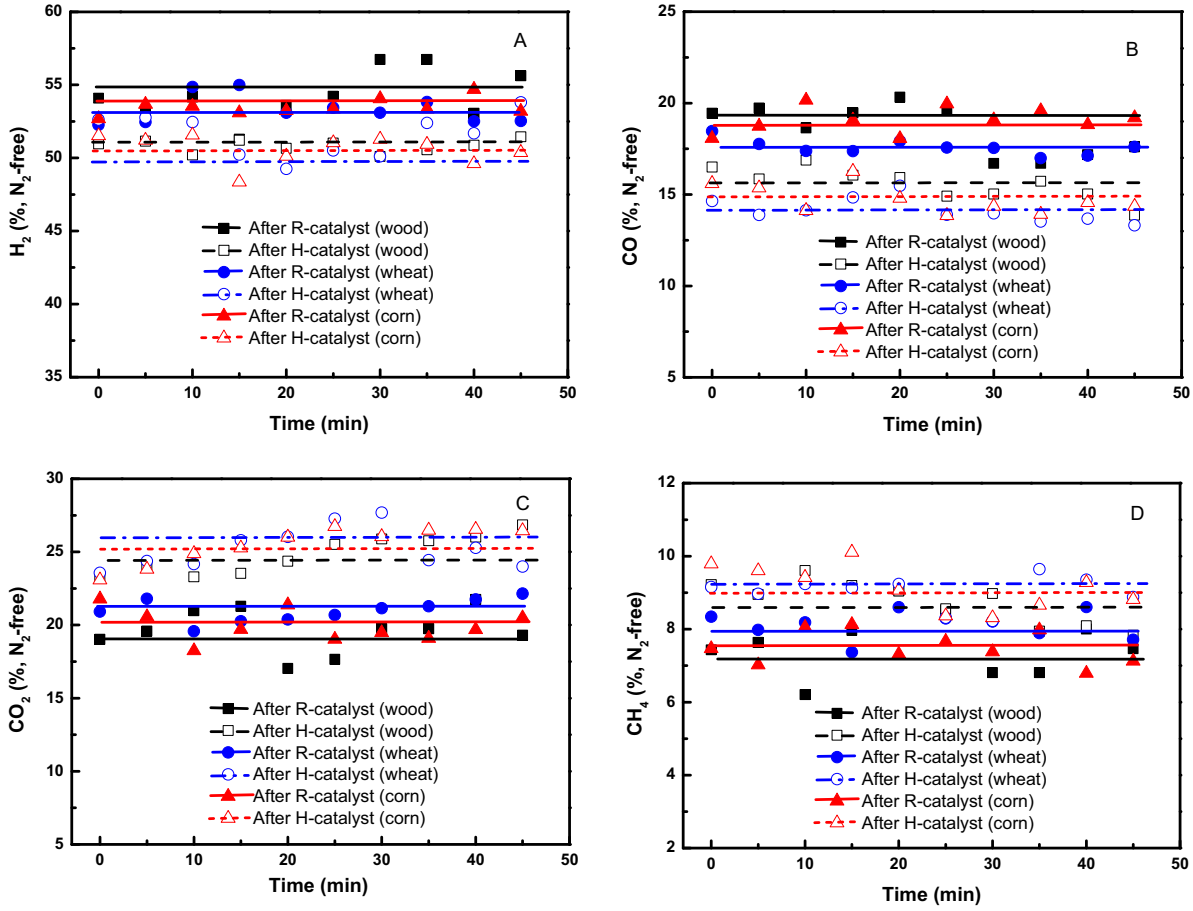

Fig. 4. Gas compositions on the dry and N_2-free basis in the presence of R-catalyst or H-catalyst using different gasification feedstock.

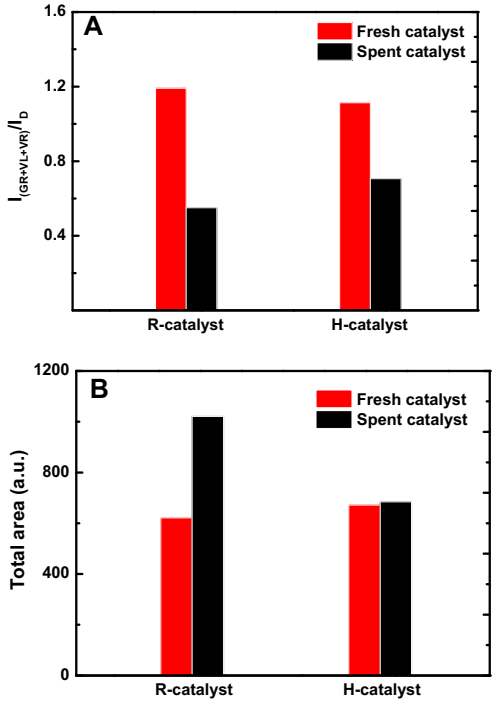

Fig. 5. FT-Raman spectral characteristics of R- and H-catalysts before and after being used. (a) Band intensity ratio of $I_{(GR+VL+VR)}/I_D$ and (b) Raman peak area.

The total Raman area of spent R-catalyst apparently increased, compared to that of fresh R-catalyst, whereas the H-catalysts could see very little changes after being used as is indicated in Fig. 5(b). Certainly, the more condensed carbon structures in the catalysts as shown in Fig. 5(a) would enable the decrease in the Raman areas of the spent catalysts. The dramatic increase in the Raman area of the spent R-catalyst should therefore result from the formation of O-containing functional groups on the char surface. The reaction between the R-catalyst and steam was faster than that between the H-catalyst and steam, which was experimentally observed by flowing steam into the catalyst chamber and monitoring the H_2 and CO production on line. The fact that the increase in O-containing complexes due to the partial gasification in steam could enhance the total Raman area was presented in [28] where the increase in the total Raman area was closely related to the extent of char-steam reactions. The limited changes in the total area for the H-catalyst before and after being used should be attributed to the comparable effects of O-containing groups and aromatisation in the catalyst.

3.3.2. Inorganic species

Fig. 6 shows the AAEM contents in R- and H-catalysts before and after being used. Na was not included as its contents were too low to see reasonable trends. Clearly, the spent H- or R-catalysts contained much more AAEM than the fresh ones, particularly K. The adsorption of AAEM in char bed has been investigated in previous studies [24,29,30]. It was believed that the chemical bonds between AAEM and chars could be formed besides physical adsorptions. In addition to the AAEM, other inorganic species in

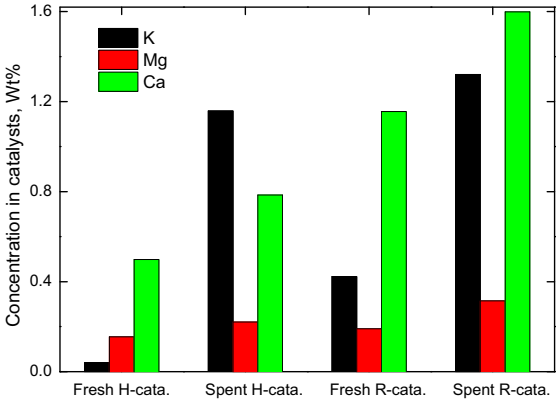

Fig. 6. The AAEM concentrations in the fresh and spent catalysts.

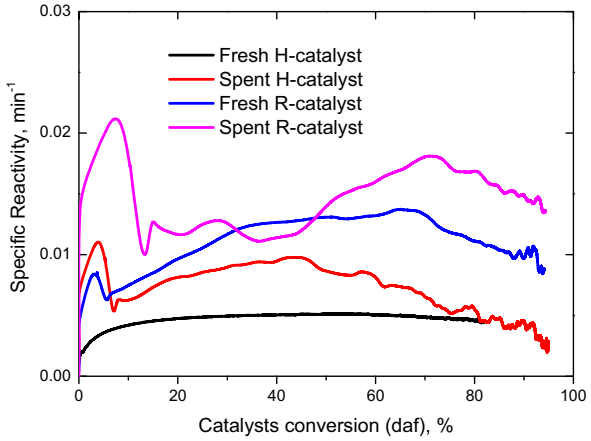

Fig. 8. Specific reactivity of fresh and spent catalysts measured at 400 °C in air using TGA.

ash could be also captured in the catalysts bed as evidenced in Fig. 7, in which the ash yields of the spent catalysts were nearly double of those of the fresh catalysts. The enrichment of inorganic species was much more than what can be expected from the consumption of char alone. These results therefore clearly demonstrate that the char catalysts can also act as the absorbent bed to remove the volatilised AAEM and other inorganic species during the gasification of biomass in the main gasifier. It must have also acted as a filter to retain the small fine particles. The increases in the AAEM (e.g. K) in the catalyst bed could not only enhance catalytic performances for tar reforming but also simultaneously mitigate the corrosion/erosion problems for the downstream use of the product gas.

3.3.3. Combustion reactivity

The fresh and spent catalysts were further analysed using TGA to compare their isothermal reactivity at various carbon conversion levels in air at the low temperature, which could reflect the combined effects of carbon structure and inorganic species on the catalysts' activity in an oxidative atmosphere. Fig. 8 shows the combustion reactivity of fresh and spent catalysts as a function of conversion at 400 °C in air. The R-catalyst containing abundant metallic species generally shows higher reactivity than the H-catalyst. In the meantime, the spent catalysts were generally more reactive to oxygen than that of fresh catalysts in most conversion ranges. Furthermore, the reactivity curves of spent catalysts fluctuated much more severely than those of fresh catalysts. The trend of fresh H-catalyst curve initially increased and then kept nearly unchanged.

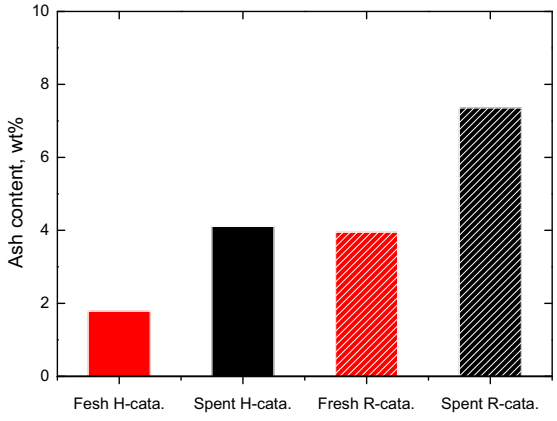

Fig. 7. Ash yields of fresh and spent catalysts.

The simple/smooth reactivity curve for the fresh H-catalyst was mainly ascribed to the lack of inorganic species. The fresh H- and R-catalysts shared very similar carbon structure as shown in Fig. 5. The concentrations of inorganic species in the catalysts would increase with increasing carbon conversion as the oxidative reaction temperature (400 °C) was too low for their release into the gas phase, leading to the increase in reactivity with increasing conversion. However, the accumulated inorganic species gradually became less catalytically effective as reactive carbon structural units were continuously removed, which was the key reason for the R-catalysts reactivity to decrease at the later stage of conversion.

After being used during the reforming process, both H- and R-catalysts showed increased combustion reactivity with waved curves. The reforming reactions could concurrently result in coke formation, AAEM deposition and carbon structure modification for the catalysts. The high values of reactivity at the initial conversion stage could be attributed to the formation of coke/soot with reactive structures on the catalyst surface, while the AAEM deposition in the catalysts bed should be the key reason for the increase in the reactivity for the spent catalysts, compared to the fresh ones. Furthermore, the fluctuating curves for the reactivity of the spent catalyst were mainly due to the highly heterogeneous biomass char structure [31], which was considerably enhanced by the reforming reactions. The radicals generated from the reforming reactions may have randomly rearranged the char structure. The variation in char (catalysts) structure could further alter the char-inorganics interactions, thus together leading to the waved curves of the spent catalyst.

4. Conclusions

The raw biomass char and acid-washed char were used as catalysts for reforming tars during the gasification of mallee wood, corn stalk and wheat straw in a pilot scale gasification plant. Based on the discussion above, the following conclusions could be drawn.

- Both the raw char and acid-washed char catalysts were very effective for reforming the tars from the gasification of various biomass feedstock. The raw char catalyst could reduce the tar contents in the product gas to a level much lower than 100 mg/N m^3, as well as increase H_2 and CO concentrations in the product gas.
- The aromatic ring systems, especially the large aromatics (no less than 3 fused rings), could be more preferentially reformed by both catalysts than the small aromatic ring systems. The

difference in the fluorescence spectra of tars after reforming with the raw and acid-washed char catalysts was consistent with the tar contents analysed using the combustion method.

- After use, the carbon structure in the catalysts became more condensed and the inorganic species contents significantly increased. The variations in carbon structure and the AAEM contents in the spent catalysts have together contributed to the high reactivity in air measured using TGA. In addition to the catalytic role for reforming tarry materials, the char catalyst bed is also acting as effective filters to arrest the volatilised AAEM species and even possibly ash fine particles from the raw gasification product gas.

Acknowledgements

This project is supported by the Commonwealth of Australia under the Australia-China Science and Research Fund and Ministry of Science and Technology (Grant No.: 2013DFG61490). This project also received funding from the Australian Government through ARENA's Emerging Renewables Program. This research used large samples of mallee biomass supplied without cost by David Pass and Wendy Hobley from their property in the West Brookton district. The authors thank Dimple Quyn for helpful discussion.

References

[1] Li C-Z. Some recent advances in the understanding of the pyrolysis and gasification behaviour of Victorian brown coal. Fuel 2007;86(12):1664–83.
[2] Li C-Z. Importance of volatile–char interactions during the pyrolysis and gasification of low-rank fuels – a review. Fuel 2013;112:609–23.
[3] Dong L, Asadullah M, Zhang S, Wang XS, Wu HW, Li C-Z. An advanced biomass gasification technology with integrated catalytic hot gas cleaning. Part I: Technology and initial experimental results in a lab-scale facility. Fuel 2013;108:409–16.
[4] Zhang S, Asadullah M, Dong L, Tay HL, Li C-Z. An advanced biomass gasification technology with integrated catalytic hot gas cleaning. Part II: Tar reforming using char as a catalyst or as a catalyst support. Fuel 2013;112:646–53.
[5] Zhang S, Min ZH, Tay HL, Asadullah M, Li C-Z. Effects of volatile–char interactions on the evolution of char structure during the gasification of Victorian brown coal in steam. Fuel 2011;90(4):1529–35.
[6] Zhang S, Hayashi JI, Li C-Z. Volatilisation and catalytic effects of alkali and alkaline earth metallic species during the pyrolysis and gasification of Victorian brown coal. Part IX. Effects of volatile-char interactions on char–H_2O and char–O_2 reactivities. Fuel 2011;90(4):1655–61.
[7] Li C-Z, Wu HW, Asadullah M, Wang XS. A method of gasifying carbonaceous material and a gasification system. International patent: WO/2012/012823 (PCT/AU2011/000936).
[8] Świerczyński D, Libs S, Courson C, Kiennemann A. Steam reforming of tar from a biomass gasification process over Ni/olivine catalyst using toluene as a model compound. Appl Catal B 2007;74(3):211–22.
[9] Caballero MA, Aznar MP, Gil J, Martin JA, Frances E, Corella J. Commercial steam reforming catalysts to improve biomass gasification with steam-oxygen mixtures. 1. Hot gas upgrading by the catalytic reactor. Ind Eng Chem Res 1997;36(12):5227–39.
[10] Simell PA, Hirvensalo EK, Smolander VT, Krause AOI. Steam reforming of gasification gas tar over dolomite with benzene as a model compound. Ind Eng Chem Res 1999;38(4):1250–7.
[11] Aznar MP, Caballero MA, Gil J, Martin JA, Corella J. Commercial steam reforming catalysts to improve biomass gasification with steam-oxygen mixtures. 2. Catalytic tar removal. Ind Eng Chem Res 1998;37(7):2668–80.
[12] Min Z, Zhang S, Yimsiri P, Wang Y, Asadullah M, Li C-Z. Catalytic reforming of tar during gasification. Part IV. Changes in the structure of char in the char-supported iron catalyst during reforming. Fuel 2013;106:858–63.
[13] Song Y, Xiang J, Hu S, Quyn DM, Zhao YJ, Hu X, et al. Importance of the aromatic structures in volatiles to the in-situ destruction of nascent tar during the volatile–char interactions. Fuel Process Technol 2015;132:31–8.
[14] Min ZH, Asadullah M, Yimsiri P, Zhang S, Wu HW, Li C-Z. Catalytic reforming of tar during gasification. Part I. Steam reforming of biomass tar using ilmenite as a catalyst. Fuel 2011;90(5):1847–54.
[15] Min ZH, Yimsiri P, Asadullah M, Zhang S, Li C-Z. Catalytic reforming of tar during gasification. Part II. Char as a catalyst or as a catalyst support for tar reforming. Fuel 2011;90(7):2545–52.
[16] Wang Y, Hu X, Song Y, Min ZH, Mourant D, Li TT, et al. Catalytic steam reforming of cellulose-derived compounds using a char-supported iron catalyst. Fuel Process Technol 2013;116:234–40.
[17] Song Y, Wang Y, Hu X, Hu S, Xiang J, Zhang L, et al. Effects of volatile–char interactions on in-situ destruction of nascent tar during the pyrolysis and gasification of biomass. Part I. Roles of nascent char. Fuel 2014;122:60–6.
[18] Song Y, Wang Y, Hu X, Xiang J, Hu S, Mourant D, et al. Effects of volatile–char interactions on in-situ destruction of nascent tar during the pyrolysis and gasification of biomass. Part II. Roles of steam. Fuel 2015;143:555–62.
[19] Quyn DM, Wu HW, Li C-Z. Volatilisation and catalytic effects of alkali and alkaline earth metallic species during the pyrolysis and gasification of Victorian brown coal. Part I. Volatilisation of Na and Cl from a set of NaCl-loaded samples. Fuel 2002;81:143–9.
[20] Quyn DM, Wu HW, Bhattacharya SP, Li C-Z. Volatilisation and catalytic effects of alkali and alkaline earth metallic species during the pyrolysis and gasification of Victorian brown coal. Part II. Effects of chemical form and valence. Fuel 2002;81:151–8.
[21] Wu HW, Quyn DM, Li C-Z. Volatilisation and catalytic effects of alkali and alkaline earth metallic species during the pyrolysis and gasification of Victorian brown coal. Part III. The importance of the interactions between volatiles and char at high temperature. Fuel 2002;81:1033–9.
[22] Sathe C, Hayashi JI, Li C-Z, Chiba T. Release of alkali and alkaline earth metallic species during rapid pyrolysis of a Victorian brown coal at elevated pressures. Fuel 2003;82:1491–7.
[23] Quyn DM, Hayashi JI, Li C-Z. Volatilisation of alkali and alkaline earth metallic species during the gasification of a Victorian brown coal in CO_2. Fuel Process Technol 2005;86:1241–51.
[24] Sonoyama N, Okuno T, Mašek O, Hosokai S, Li C-Z, Hayashi JI. Interparticle desorption and re-adsorption of alkali and alkaline earth metallic species within a bed of pyrolyzing char from pulverized woody biomass. Energy Fuels 2006;20(3):1294–7.
[25] Quyn DM, Wu HW, Hayashi JI, Li C-Z. Volatilisation and catalytic effects of alkali and alkaline earth metallic species during the pyrolysis and gasification of Victorian brown coal. Part IV. Catalytic effects of NaCl and ion-exchangeable Na in coal on char reactivity. Fuel 2003;82(5):587–93.
[26] Bridgwater AV. The technical and economic feasibility of biomass gasification for power generation. Fuel 1995;74(5):631–53.
[27] Bhattacharya SC, Mizanur Rahman Siddique AHM, Pham HL. A study on wood gasification for low-tar gas production. Energy 1999;24:285–96.
[28] Tay HL, Kajitani S, Zhang S, Li C-Z. Effects of gasifying agent on the evolution of char structure during the gasification of Victorian brown coal. Fuel 2013;103:22–8.
[29] Okuno T, Sonoyama N, Hayashi JI, Li C-Z, Sathe C, Chiba T. Primary release of alkali and alkaline earth metallic species during the pyrolysis of pulverized biomass. Energy Fuels 2005;19(5):2164–71.
[30] Sathe C, Hayashi JI, Li C-Z, Chiba T. Combined effects of pressure and ion-exchangeable metallic species on pyrolysis of Victorian lignite. Fuel 2003;82(3):343–50.
[31] Asadullah M, Zhang S, Min Z, Yimsiri P, Li C-Z. Effects of biomass char structure on its gasification reactivity. Bioresour Technol 2010;101(20):7935–43.